Inorg. Chem. **2006**, *45*, 5653–5660

Increasing the Ordering Temperatures in Oxalate-Based 3D Chiral Magnets: the Series $[Ir(ppy)_2(bpy)][M^{II}M^{III}(ox)_3]\cdot 0.5H_2O$ ($M^{II}M^{III}$ = MnCr, FeCr, CoCr, NiCr, ZnCr, MnFe, FeFe); bpy = 2,2′-Bipyridine; ppy = 2-Phenylpyridine; ox = Oxalate Dianion)

Miguel Clemente-León,* Eugenio Coronado,* Carlos J. Gómez-García, and Alejandra Soriano-Portillo

Instituto de Ciencia Molecular, Universidad de Valencia, Polígono de la Coma s/n, 46980 Paterna, Spain

Received March 15, 2006

The synthesis, structure, and physical properties of a novel series of oxalate-based bimetallic magnets obtained by using the $Ir(ppy)_2(bpy)]^+$ cation as a template of the bimetallic $[M^{II}M^{III}(ox)_3]^-$ network are reported. The compounds can be formulated as $[Ir(ppy)_2(bpy)][M^{II}Cr^{III}(ox)_3]\cdot 0.5H_2O$ (M^{II} = Ni, Mn, Co, Fe, and Zn) and $[Ir(ppy)_2(bpy)][M^{II}Fe^{III}(ox)_3]\cdot 0.5H_2O$ (M^{II} = Fe, Mn) and crystallize in the chiral cubic space group $P4_132$ or $P4_332$. They show the well-known 3D chiral structure formed by M^{II} and M^{III} ions connected through oxalate anions with $[Ir(ppy)_2(bpy)]^+$ cations and water molecules in the holes left by the oxalate network. The $M^{II}Cr^{III}$ compounds behave as soft ferromagnets with ordering temperatures up to 13 K, while the $Mn^{II}Fe^{III}$ and $Fe^{II}Fe^{III}$ compounds behave as a weak ferromagnet and a ferrimagnet, respectively, with ordering temperatures of 31 and 28 K. These values represent the highest ordering temperatures so far reported in the family of 3D chiral magnets based on bimetallic oxalate complexes.

Introduction

The octahedral tris(oxalato) metalate complexes $[M(ox)_3]^{3-}$ ($M = Cr^{III}$, Fe^{III}, Ru^{III}) can be assembled with divalent metal cations to build heterobimetallic extended networks. The interest of this kind of compounds started with the discovery of ferro- and ferrimagnetism in the bimetallic layered oxalate-bridged compounds of general formula $A[M^{II}M^{III}(ox)_3]$ (A = tetraalkylamonium derivative) that present ordering magnetic temperatures between 6 and 45 K.[1] These compounds present a 2D honeycomb-layered structure.[2] The role of the bulky "A" cations is to act as templates stabilizing the formation of the anionic oxalate layers. Taking advantage of the layered structure of these oxalate-based magnets, different electroactive cations have been introduced between the oxalate layers leading to multifunctional magnetic materials. Some interesting examples are the insertion of decamethylferrocenium cations,[3] photochromic molecules,[4] NLO-active molecules,[5] and organic π-electron donors.[6−8] This last combination provides the first example of coexistence in the same molecular material of ferromagnetism and metallic conductivity.[6]

A second type of bimetallic network is formed when the templating cations are chiral metallic complexes such as $[Z^{II}(bpy)_3]^{2+}$ (Z = Ru, Fe, Co, Zn, Ni). This 3D structure presents a chiral cubic packing.[9] The general formulas of

* To whom correspondence should be addressed. E-mail: miguel.clemente@uv.es (M.C.-L.); eugenio.Coronado@uv.es (E.C.). Tel: (+34) 96 3544415 (M.C.-L.). Fax: (+34) 96 354 3273 (M.C.-L.).

(1) (a) Tamaki, H.; Zhong, Z. J.; Matsumoto, N.; Kida, S.; Koikawa, M.; Achiwa, N.; Hashimoto, Y.; Okawa, H. *J. Am. Chem. Soc.* **1992**, *114*, 6974. (b) Tamaki, H.; Mitsumi, M.; Nakamura, N.; Matsumoto, N.; Kida, S.; Okawa, H.; Ijima, S. *Chem. Lett.* **1992**, 1975. (c) Mathonière, C.; Carling, S. G.; Yuscheng, D.; Day, P. *J. Chem. Soc., Chem. Commun.* **1994**, 1551. (d) Mathonière, C.; Nutall, J.; Carling, S. G.; Day, P. *Inorg. Chem.* **1996**, *35*, 1201. (e) Min, K. S.; Rhinegold, A. L.; Miller, J. S. *Inorg. Chem.* **2005**, *44*, 8433.

(2) Pellaux, R.; Schmalle, H. W.; Huber, R.; Fisher, P.; Hauss, T.; Ouladdiaf, B.; Decurtins, S. *Inorg. Chem.* **1997**, *36*, 2301.

(3) (a) Coronado, E.; Galán-Mascarós, J. R.; Gómez-García, C. J.; Ensling, J.; Gutlich, P. *Chem. Eur. J.* **2000**, *6*, 552. (b) Coronado, E.; Galán-Mascarós, J. R.; Gómez-García, C. J.; Martínez-Agudo, J. M. *Adv. Mater.* **1999**, *11*, 558. (c) Clemente-León, M.; Galán-Mascarós, J. R.; Gómez-García, C. J. *Chem. Commun.* **1997**, 1727.

(4) Bénard, S.; Yu, P.; Audière, J. P.; Rivière, E.; Clèment, R.; Ghilhem, J.; Tchertanov, L.; Nakatami, K. *J. Am. Chem. Soc.* **2000**, *122*, 9444.

(5) Bénard, S.; Rivière, E.; Yu, P.; Nakatami, K.; Delouis, J. F. *Chem. Mater.* **2001**, *13*, 159.

(6) Coronado, E.; Galán-Mascarós, J. R.; Gómez-García C. J.; Laukhin, V. *Nature* **2000**, *408*, 447.

(7) Alberola, A.; Coronado, E.; Galán-Mascarós, J. R.; Giménez-Saiz, C.; Gómez-García, C. J. *J. Am. Chem. Soc.* **2003**, *125*, 10774.

(8) Coronado, E.; Galán-Mascarós, J. R.; Gómez-García, C. J.; Martínez-Ferrero, E.; Van Smaalen, S. *Inorg. Chem.* **2004**, *43*, 4808.

10.1021/ic060442x CCC: $33.50
Published on Web 06/15/2006

this class of compounds are $[Z(bpy)_3]X[MM'(ox)_3]$[10,11] and $[Ru(ppy)(bpy)_2][MM'(ox)_3]$[12] (Z = Ru, Fe, Co and Ni; X = ClO_4^-, BF_4^-, PF_6^-; M, M′ = Li^I, Na^I, Mn^{II}, Ni^{II}, Co^{II}, Fe^{II}, Cu^{II}, Zn^{II}, Rh^{III}, Co^{III}, Cr^{III}, and Fe^{III}; bpy = bipyridine, ppy = phenylpyridine). In contrast to 2D compounds, which admit a large variety of cations, in the 3D structures, the templating cation must have the appropriate symmetry (D_3), size, and charge. Another characteristic feature of these 3D compounds is that all their metal centers have the same chirality, while in the 2D structure, the adjacent metal centers exhibit alternated chirality. Chirality plays a crucial role in this molecular recognition process. Thus, chiral tris(bipyridine) metal cations induce the spontaneous resolution of 3D chiral lattices with the same configuration as the tris(oxometalate) sites. With this strategy, enantiomerically pure compounds of formulas $[Ru(bpy)_3][LiCr(ox)_3]$,[13] $[Ru(bpy)_3][ClO_4][MnCr(ox)_3]$, $[Ru(ppy)(bpy)_2][M^{II}Cr^{III}(ox)_3]$ (M = Ni, Mn,),[14] and $[Ru(bpy)_3][Cu_{2x}Ni_{2(2-x)}(ox)_3]$[12] have been prepared in which crossing effects (magnetochiral dichroism) may arise from the combination of magnetism and chirality. Another interesting result obtained in this family is the presence of a thermal spin transition in $[Co(bpy)_3][LiCr(ox)_3]$.[15] From the magnetic point of view, the chiral compounds leading to ordered magnetic phases are the homometallic series $[M^{II}M^{II}]$ that behave as antiferromagnets or weak ferromagnets[16] and the bimetallic series $[M^{II}M^{III}]$ reported by our group that behave as ferro-, weak ferro-, and ferrimagnets as the analogous 2D compounds but with lower ordering temperatures.[11,17] This lower ordering temperature indicates that, despite the higher dimensionality of this type of compounds, they present weaker magnetic exchange interactions due to the different relative orientation of the magnetic orbitals and also to the longer metal-to-metal distances.

In this paper, we present a successful extension of the 3D oxalate series using the diamagnetic $[Ir(ppy)_2(bpy)]^+$ cation as a templating complex. This choice is justified by the fact that the charge and size of this cation are different from those of the $[Z(bpy)_3]^{2+}$ complexes previously used to prepare the chiral magnets $[Z(bpy)_3][ClO_4][M^{II}M^{III}(ox)_3]$.[11] In particular, due to its lower charge (+1), the perchlorate anion is not needed in the structure. This fact could provide the opportunity of studying the structural changes caused by the introduction of this templating complex in the 3D oxalate network, as well as the changes caused in the magnetic properties by the different chemical pressure. An additional interest of the $[Ir(ppy)_2(bpy)]^+$ complex deals with its luminescence properties.[18] The incorporation of this electroactive complex inside the bimetallic oxalate framework may provide the opportunity to study the interplay between optical and magnetic properties in this system.

We report here the preparation, structural characterization, and magnetic study of the compounds of formulas $[Ir(ppy)_2(bpy)][M^{II}M^{III}(ox)_3]\cdot 0.5H_2O$ (M^{II} = Ni, Mn, Co, Fe, and Zn, M^{III} = Cr and Fe).

Experimental Section

Synthesis. The complex $[Ir(ppy)_2(bpy)]Cl$ was prepared according to literature methods.[18] $Ag_3[Cr(ox)_3]$ and $Tl_3[Fe(ox)_3]$ were prepared by metathesis from the corresponding potassium salts.[19] All other materials and solvents were commercially available and used without further purification.

$[Ir(ppy)_2(bpy)][M^{II}Cr(ox)_3]\cdot 0.5H_2O$ (M^{II} = Mn, Co, Fe, and Zn). $MCl_2\cdot 4H_2O$ (0.114 mmol) was added to a suspension of $Ag_3[Cr(ox)_3]$ (0.052 g, 0.076 mmol) in 5 mL of methanol. The AgCl precipitate was filtered, and then the clear solution was added dropwise to a solution of $[Ir(ppy)_2(bpy)]Cl$ (0.05 mg, 0.076 mmol) in 5 mL of methanol. After the mixture was stirred for 30 min, a yellow precipitate was collected by centrifugation and washed with methanol, dichloromethane, and water. Single crystals of the $[Ir(ppy)_2(bpy)][MnCr(ox)_3]\cdot 0.5H_2O$ compound were obtained by an analogous procedure by slow diffusion of both solutions on a H-tube after 3 weeks.

$[Ir(ppy)_2(bpy)][NiCr(ox)_3]\cdot 0.5H_2O$. $NiCl_2\cdot 6H_2O$ (0.077 mg, 0.324 mmol) was added to a suspension of $Ag_3[Cr(ox)_3]$ (0.15 g, 0.228 mmol) in 15 mL of methanol. The AgCl precipitate was filtered, and then the clear solution was added dropwise to a solution of $[Ir(ppy)_2(bpy)]Cl$ (0.15 mg, 0.228 mmol) in 15 mL of methanol. This solution was refluxed for 1 h. A yellow precipitate was collected by filtration and washed with methanol, dichloromethane, and water.

$[Ir(ppy)_2(bpy)][M^{II}Fe(ox)_3]\cdot 0.5H_2O$ (M^{II} = Fe and Mn). $Tl_3[Fe(ox)_3]$ (0.157 g, 0.17 mmol) was added to a solution of $MCl_2\cdot 4H_2O$ (0.255 mmol) in 5 mL of methanol. The TlCl precipitate was filtered. In a separate beaker, $Tl_3[Fe(ox)_3]$ (0.079 g, 0.085 mmol) was added to a solution of $[Ir(ppy)_2(bpy)]Cl$ (0.176 g, 0.255 mmol) in a mixture of 15 mL of methanol and 15 mL of dimethylformamide. The TlCl precipitate was filtered. The first solution was added dropwise to the second solution. After the mixture was stirred for 30 min, an orange precipitate was collected by filtration and washed with methanol.

Single crystals of the $[Ir(ppy)_2(bpy)][MnFe(ox)_3]\cdot 0.5H_2O$ compound were obtained by an analogous procedure to that of the $[Ir(ppy)_2(bpy)][MnCr(ox)_3]\cdot 0.5H_2O$ compound using $Tl_3[Fe(ox)_3]$ instead of $Ag_3[Cr(ox)_3]$.

The composition of all samples was checked by microanalysis. These measurements showed that the $Ir/M^{II}/M^{III}$ ratios are 1:1:1.

(9) Decurtins, S.; Schmalle, H. W.; Schneuwly, P.; Oswald, H. R. *Inorg. Chem.* **1993**, *32*, 1888.
(10) Decurtins, S.; Schmalle, H. W.; Schneuwly, P.; Ensling, J.; Gütlich, P. *J. Am. Chem. Soc.* **1994**, *116*, 9521.
(11) Coronado, E.; Galán-Mascarós, J. R.; Gómez-García, C. J.; Martínez-Agudo, J. M. *Inorg. Chem.* **2001**, *40*, 113.
(12) Pointillart, F.; Train, C.; Gruselle, M.; Villain, F.; Schmalle, H. W.; Talbot, D.; Gredin, P.; Decurtins, S.; Verdaguer, M. *Chem. Mater.* **2004,** *16*, 832.
(13) Andrés, R.; Gruselle, M.; Malézieux, B.; Verdaguer, M.; Vaissermann, J.; *Inorg. Chem.* **1999**, *38*, 4637.
(14) Andrés, R.; Brissard, M.; Gruselle, M.; Train, C.; Vaissermann, J.; Malézieux, B.; Jamet, J. P.; Verdaguer, M. *Inorg. Chem.* **2001**, *40*, 4633.
(15) Sieber, R.; Decurtins, S.; Stoeckli-Evans, H.; Wilson, C.; Yufit, D.; Howard, J. A. K.; Capelli, S. C.; Hauser, A. *Chem. Eur. J.* **2000**, *6*, 361.
(16) Hernández-Molina, M.; Lloret, F.; Ruiz-Pérez, C.; Julve, M. *Inorg. Chem.* **1998**, *37*, 4131.
(17) Coronado, E.; Galán-Mascarós, J. R.; Gómez-García, C. J.; Martínez-Ferrero, E.; Almeida, M.; Waerenborgh, J. C. *Eur. J. Inorg. Chem.* **2005**, *11*, 2064.
(18) Oshawa, Y.; Sprouse, S.; King, K. A.; DeArmond, M. K.; Hanck, K. W.; Watts, R. J. *J. Phys. Chem.* **1987**, *91*, 1047.
(19) Baylar, J. C.; Jones, E. M. In *Inorganic Synthesis*; Booth, H. S., Ed.; McGraw-Hill: New York, 1939; Vol. 1, p 35.

Table 1. Unit Cell Parameters for the Series $[Ir(ppy)_2(bpy)][M^{II}M^{III}(ox)_3]\cdot 0.5H_2O$

$M^{II}M^{III}$	a (Å)
MnCr[a]	15.436(6)
FeCr	15.30(5)
CoCr	15.34(2)
NiCr	15.26(4)
ZnCr	15.28(6)
FeFe	15.32(4)
MnFe[a]	15.483(6)

[a] Single-crystal data at 180 K.

Structural Characterization. Yellow prismatic single crystals of $[Ir(ppy)_2(bpy)][MnCr(ox)_3]\cdot 0.5H_2O$ and $[Ir(ppy)_2(bpy)][MnFe(ox)_3]\cdot 0.5H_2O$ were collected and mounted on a nonius KappaCCD diffractometer equipped with graphite-monochromated Mo K_α radiation ($\lambda = 0.71073$ Å). X-ray diffraction data were collected at 180 K. The denzo and Scalepack programs were used for cell refinements and data reduction.[20] The structures were solved by direct methods using the SIR97 program[21] and refined on F^2 with the SHELX-97 program.[22] The Flack's absolute parameter (x) was used to determine the space group of the two compounds.[23] Both compounds exhibit a x parameter close to 0. This parameter lies within the range that indicates that the absolute structure is valid and that the two crystals are enantiopure.[23] All non-hydrogen atoms were refined anisotropically. The water molecule was found to be disordered with an occupancy factor of 0.5. Crystallographic data for the structures reported in this paper have been deposited with the Cambridge Crystallographic Data Center as supplementary publications no. CCDC 270162 and CCDC 270163. Copies of the data can be obtained free of charge on application to CCDC, 12 Union Road, Cambridge CB21EZ, UK (fax: (+44) 1223-336-033; e-mail: deposit@ccdc.cam.ac.uk).

X-ray powder patterns were collected with a Siemens D-500 X-ray diffractometer (Cu K_α radiation, $\lambda_\alpha = 1.54184$ Å) at room temperature. The powder diffraction patterns indicate that all compounds are isostructural and show analogous patterns to the simulated patterns from the atomic coordinates of the crystal structures of $[Ir(ppy)_2(bpy)][MnCr(ox)_3]\cdot 0.5H_2O$ and $[Ir(ppy)_2(bpy)][MnFe(ox)_3]\cdot 0.5H_2O$ (see Supporting Information).[24] Indexation of the main reflections gave the unit cell parameters shown in Table 1.

Physical Measurements. Magnetic susceptibility measurements were performed on polycrystalline samples using a magnetometer (Quantum Design MPMS-XL-5) equipped with a SQUID sensor. Variable-temperature measurements were carried out in the temperature range 2−300 K. The ac measurements were performed in the range 2−20 K at different frequencies with an oscillating magnetic field of 0.395 mT. The magnetization and hysteresis studies were performed between 5 and −5 T, cooling the samples at zero field. Magnetization and hysteresis studies of $[Ir(ppy)_2(bpy)][MnCr(ox)_3]\cdot 0.5H_2O$ and $[Ir(ppy)_2(bpy)][FeFe(ox)_3]\cdot 0.5H_2O$ were performed between 9 and −9 T with a Quantum Design PPMS. Calorimetric measurements were performed on pressed pellets with a Quantun Design PPMS-9 in the range 2−40 K. The $Ir/M^{II}/M^{III}$ ratios were measured on a Philips ESEM ×230 scanning electron microscope equipped with an EDAX DX-4 microsonde.

Results and Discussion

Synthesis and Structure. The method used to prepare $[Ir(ppy)_2(bpy)][M^{II}M^{III}(ox)_3]\cdot 0.5H_2O$ (M^{II} = Mn, Co, Fe, and Zn, M^{III} = Cr and Fe) is analogous to that used to prepare the other oxalate-based 3D $[M^{II}M^{III}(ox)_3]$ compounds with $[Z(bpy)_3]^{2+}$ (Z^{II} = Ru, Fe, Co, and Ni) cations.[11] This synthesis is based in the use of $Ag_3[Cr(ox)_3]$ to avoid the presence of alkali ions in the structure. Crystals of good quality for X-ray diffraction analysis of the MnCr derivative were grown by slow diffusion in methanol. The structure of this compound was solved by single-crystal X-ray diffraction. All other $M^{II}Cr^{III}$ compounds were obtained as fine powders by direct precipitation. X-ray powder diffraction of these compounds indicate that all are isostructural (see Table 1). In the case of the NiCr derivative, it was necessary to change the synthetic procedure. A yellow powder of this derivative was obtained using the same conditions but with 1 h reflux. Single crystals of MnFe suitable for X-ray diffraction were also obtained by slow diffusion in methanol using $Tl_3[Fe(ox)_3]$. These crystals were obtained in very low yield mixed with some impurities. To perform the magnetic characterization of MnFe and to synthesize FeFe, powder samples of these two derivatives were obtained by direct precipitation that were found to be isostructural by X-ray powder diffraction. In these two cases, the synthetic procedure was changed to get more pure samples. The main differences with respect to the synthesis of the $M^{II}Cr^{III}$ series are the use of a dimethylformamide/methanol mixture as solvent and the use of a $Ir/M^{II}/Fe^{III}$ ratio of 1:1:1 instead of the $Ir/M^{II}/Cr^{III}$ ratio 1:1.5:1.

As in the 3D oxalate analogues,[9−11] all these iridium-based compounds crystallize in the cubic space group $P4_132$ or $P4_332$, depending of the chirality. The structures of MnFe and MnCr were solved for crystals of opposite chirality. The two compounds present the well-known 3D three-connected decagon oxalate-based anionic network (10,3) which is formed by oxalate ligands connecting M^{II} and M^{III} ions in such a way that each M^{II} is surrounded by three M^{III} and vice versa with all metal ions presenting the same chirality (Figure 1). Both metals are crystallographically equivalent with mean M−O distances of 2.112(7) and 2.130(6) Å for the MnFe compound and 2.102(8) and 2.128(9) Å for the MnCr compound. Those distances are intermediate between the ones expected for Fe^{III}−O and Mn^{II}−O and Cr^{III}−O and Mn^{II}−O, respectively. Metal−metal distances are 5.503 Å in the MnCr compound and 5.524 Å in the MnFe compound. These metal−metal distances are significantly shorter than those exhibited by the $[Ru(bpy)_3]^{2+}$ analogues. For example, in the MnCr compound, this value is shortened from 5.548 to 5.503 Å.[11] This shortening is also reflected in the unit cell parameters calculated from X-ray powder diffraction data of the other compounds of the $[Ir(ppy)_2(bpy)]^+$ family (see Tables 1 and 2).

In the structure, the bimetallic oxalate networks are stabilized by the presence of $[Ir(ppy)_2(bpy)]^+$ cations of the

(20) Otwinowski, Z.; Minor, W. In *Methods in Enzymology*; Carter, C. W., Jr., Sweet, R. M., Eds.; Academic Press: New York, 1997; Vol. 276, p 307.
(21) *SIR97*: Altomare, A.; Burla, M. C.; Camali, M.; Cascarano, G. L.; Giacovazzo, C.; Guagliardi, A.; Moliterni, A. G. G.; Polidori, G.; Spagna, R. *J. Appl. Crystallogr.* **1999**, *32*, 115.
(22) Sheldrick, G. M. *SHELXL-97*; University of Göttingen: Göttingen, Germany, 1997.
(23) Flack, H. D.; Bernardinelli, G. *J. Appl. Crystallogr.* **2000**, *33*, 1143.
(24) *CrystalDiffract 4.0.2* (CrystalMaker software).

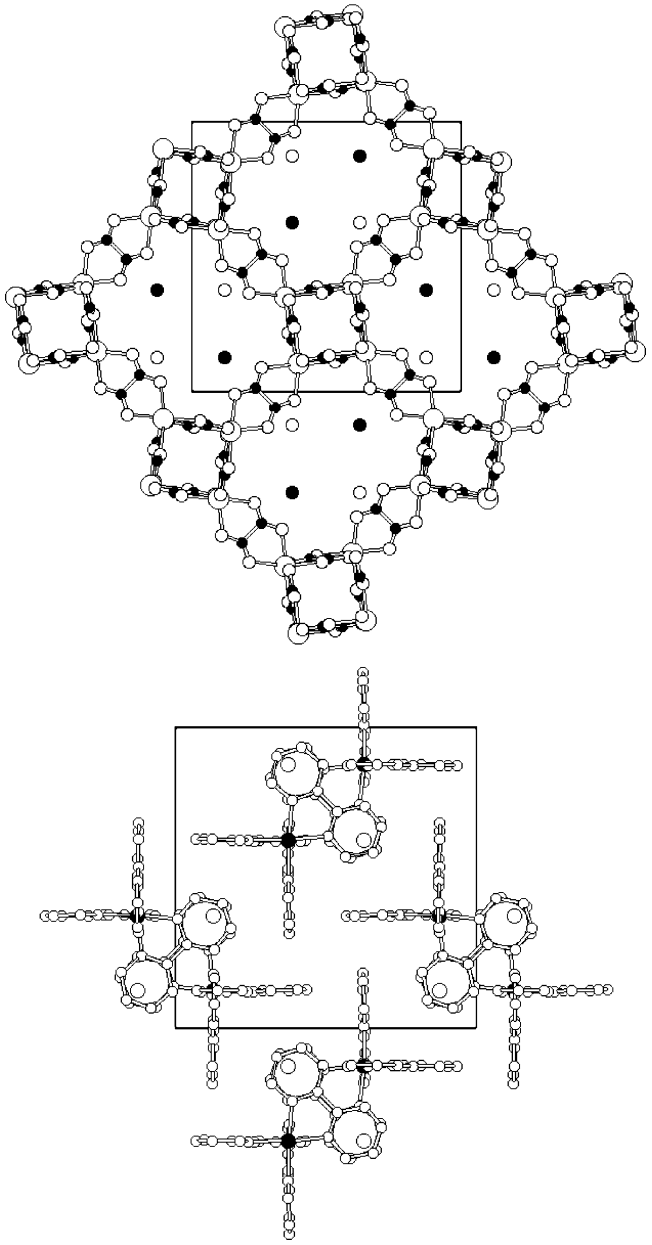

Figure 1. Projection on the *ab* plane of the structure of $[Ir(ppy)_2(bpy)][MnFe(ox)_3]\cdot 0.5H_2O$. Only the Ir atoms (in black) and the water molecules (in white) are drawn in the cavities (top). Projection of the $[Ir(ppy)_2(bpy)]^+$ cations and water molecules in the same structure (bottom).

Table 2. Unit Cell and Magnetic Parameters for the Series $[Z^{II}(bpy)_3][ClO_4][M^{II}M^{III}(ox)_3]$[11,17]

$Z^{II}M^{II}M^{III}$	a (Å)	T_c (K)	$Z^{II}M^{II}M^{III}$	a (Å)	T_c (K)
RuMnCr	15.506(2)	<2	NiMnCr	15.45(4)	2.3
RuFeCr	15.46(3)	2.5	NiFeCr	15.44(6)	4.0
RuCoCr	15.51(4)	2.8	CoMnCr	15.49(5)	2.2
RuNiCr	15.40(8)	6.4	RuMnFe	15.48(4)	17.4
FeMnCr	15.43(4)	3.9	FeMnFe	15.39(3)	20.0
FeFeCr	15.30(5)	4.7	RuFeFe	15.44(4)	7.9
FeCoCr	15.38(6)	6.6	FeFeFe	15.33(2)	9.1

appropriate chirality (Figure 1). The space group requires a single coordination distance (Ir−N or Ir−C) around the metal of 2.062(10) Å. This means that the two ppy ligands and the bpy ligand are randomly distributed around each Ir atom. The presence of ppy or bpy is not directly pointed out by the X-ray structure, but it is undoubtedly confirmed by the

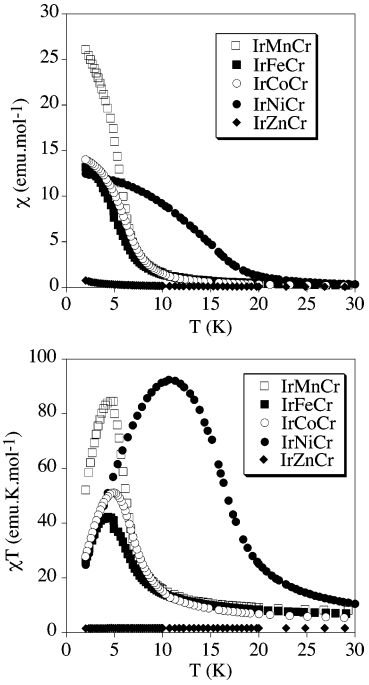

Figure 2. Temperature dependence of the magnetic susceptibility at 0.1 T (χ) for the IrMCr series (top). Temperature dependence of the χT product at 0.1 T for the IrMCr series (bottom).

absence of free $[ClO_4]^-$ anions. While in the $[Z(bpy)_3]^{2+}$ family of bimetallic oxalate-based magnets, the $[ClO_4]^-$ anions occupy the holes left by the cation complexes and counterbalance their cationic charge, in the $[Ir(ppy)_2(bpy)]^+$ family, the holes left by the cationic complexes are occupied by a disordered water molecule with an occupancy factor of 1/2. This is the reason the unit cell parameters of the $[Ir(ppy)_2(bpy)]^+$ family of bimetallic oxalato-based magnets are smaller than those exhibited by the $[Z(bpy)_3]^{2+}$ family (see Table 2). The $[Ru(ppy)(bpy)_2][MnCr(ox)_3]$ compound, which is the other known compound containing a monocation inside the 3D oxalate network, presents also a smaller unit cell than the analogous $[Ru(bpy)_3][ClO_4][MnCr(ox)_3]$ compound (a = 15.368(5) Å).[14] This shortening can be also explained by the absence of $[ClO_4]^-$ anions. As expected, the unit cell of this compound is also smaller than that of the $[Ir(ppy)_2(bpy)][MnCr(ox)_3]\cdot 0.5H_2O$ compound since the $[Ru(ppy)(bpy)_2]^+$ cation is smaller than the $[Ir(ppy)_2(bpy)]^+$ cation.

Magnetic Properties. Cr(III) Series: $[Ir(ppy)_2(bpy)][M^{II}Cr^{III}(ox)_3]\cdot 0.5H_2O$ (M^{II} = Ni, Mn, Co and Fe). Figure 2 (top) shows the temperature dependence of the magnetic susceptibility (χ) of the $M^{II}Cr^{III}$ compounds. In all cases, the magnetic susceptibility follows a Curie−Weiss law in the range 50−300 K. The resulting parameters are summarized in Table 3. Positive parameters of the Weiss constants are obtained for all the compounds. This indicates the presence of ferromagnetic interactions between neighboring $M^{II}-Cr^{III}$ magnetic ions. This is confirmed by the gradual increase of the χT product upon cooling (Figure 2, bottom). At room temperature, the observed value of χT is approximately equal to the sum of the expected contributions of the isolated paramagnetic ions. At low temperatures, all the samples

Table 3. Magnetic Parameters for the Series $[Ir(ppy)_2(bpy)][M^{II}M^{III}(ox)_3]\cdot 0.5H_2O$

$M^{II}M^{III}$	T_c (K)	θ (K)	C (emu·K/mol)	$C_{spin-only}$ (emu·K/mol)	M (μ_B) at 5 T	H_{coer} (mT) at 2 K
MnCr	5.1	6.1	6.46	6.25	7.4	2
FeCr	5.0	6.1	5.29	4.89	4.9	4
CoCr	5.2	5.2	3.98	3.75	4.1	5
NiCr	13.0	15.7	2.83	2.88	4.1	3
ZnCr		−0.8	1.67	1.88	2.5	
FeFe	28.0	−79.1	8.27	7.375	1.4	30
MnFe	31.0	−93.6	8.46	8.75	0.8	24

exhibit a sharp increase of both χ and χT. These features suggest the onset of long-range ferromagnetic ordering, as observed for the $[Ru(bpy)_3]^{2+}$ compounds.[11] Note that the temperatures at which this sharp increase appears are higher than those observed for the corresponding $[Ru(bpy)_3]^{2+}$ derivatives.[11] To confirm the presence of long-range magnetic ordering and to determine precisely the critical temperatures, ac susceptibility measurements were carried out. As expected for a sample presenting an ordered state, a maximum in the in-phase signal (χ') near T_c and an out-of-phase signal (χ'') that starts to appear at temperatures just below T_c have been observed for all these compounds (Figure 3). From these data, the T_c's of the MnCr, FeCr, CoCr, and NiCr compounds are 5.1, 5.0, 5.2, and 13.0 K, respectively. These values are around twice those of the $[Ru(bpy)_3]^{2+}$ analogues and similar to those reported for the compounds MnCr and NiCr of the $[Ru(ppy)(bpy)_2]^+$ series.[14]

Another interesting feature in the ac measurements comes from the frequency dependence of the signals. Thus, all samples show a sharp increase in χ'' below T_c and a peak at lower temperatures which is almost frequency-independent, as expected for a ferromagnet (Figure 4). However, in the ordered phase, an additional peak which is frequency-dependent is observed for CoCr and NiCr, while in the MnCr sample, χ'' shows an increase below 3 K and the peak cannot be observed, as it should appear at temperatures below 2 K. The presence of such a frequency-dependent peak in χ'' has already been observed in other low-dimensional magnets such as, for example, the 2D MnCr oxalate magnets and some 2D bimetallic cyanide complexes.[3,25] It can be related to the formation of magnetic domains and domain-wall movement.[26] In fact, an Arrhenius plot ($\ln \theta$ vs T^{-1}) of these peaks shows straight lines whose slopes allow the determination of the activation energies of this process (175 K for CoCr and 343 K for NiCr).

To confirm the ferromagnetic ordering of the spins in these compounds, isothermal magnetization at 2 K has been performed. The compounds present a sharp increase at low fields which is much faster than that expected for noninteracting M^{III} and M^{II} centers; this increase is more gradual at higher fields, and no saturation is reached up to 5 T, although the M values are close to those expected for a parallel alignment of the spins (Figure 5). For instance, the value for the MnCr compound at 5 T is 7.4 μ_B, which is slightly lower than the expected spin-only saturation value of 8 μ_B. This behavior has also been observed in the 2D and 3D series and has been attributed to a spin canting of the ferromagnetic phase.[3,11] If we compare with the analogous 3D $[Z(bpy)_3]^{2+}$ compounds, we observe that the increase of magnetization with the magnetic field is much faster in the $[Ir(ppy)_2bpy]^+$ compounds. This is a consequence of the higher T_c's of these compounds. The hysteresis loops at 2 K show that these compounds are very soft ferromagnets with coercive fields of a few millitesla (see Table 3), although these values are slightly higher that those observed in the $[Ru(bpy)_3]^{2+}$ analogues. For instance, the iridium derivative of the CoCr compound presents a coercive field of 5 mT, whereas for the analogues of ruthenium, this value is 0.8 mT.[11]

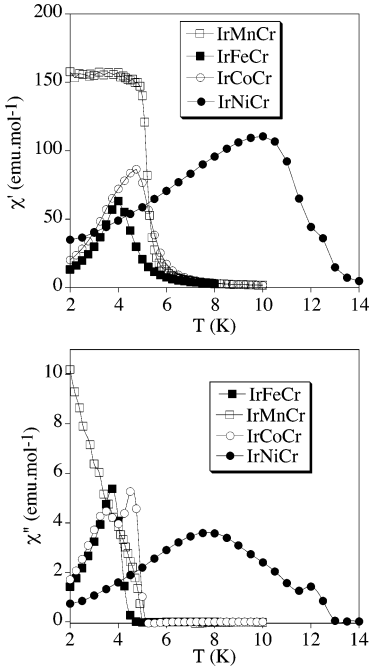

Figure 3. Temperature dependence of the in-phase ac susceptibility (χ) for the IrMCr series at 10 Hz (top). Temperature dependence of the out-of-phase ac susceptibility (χ'') for the IrMCr series at 10 Hz (bottom).

An extra confirmation of the long-range ordering observed in these compounds comes from the heat capacity measurements. These measurements were done for single crystals of the IrMnCr compound (see Supporting Information) and show peaks at temperatures very close to those observed in the dc and ac magnetic measurements.

To finish this part, we have examined the magnetic properties of the ZnCr derivative. This compound behaves as a paramagnet exhibiting the properties of isolated Cr^{III} ions. Thus, the thermal variation of the χT product shows a constant value (Figure 2) which is equal to the expected value for Cr^{III}, and the field dependence of the magnetization follows a Brillouin function for a $S = 3/2$ (see Supporting Information). This result demonstrates that inside the bimetallic oxalato framework the two metals are ordered in such a way that each Cr^{III} center is surrounded by three nonmagnetic Zn centers.

Fe(III) Series: $[Ir(ppy)_2(bpy)][M^{II}Fe(ox)_3]\cdot 0.5H_2O$ (M^{II} = Fe and Mn). The magnetic properties of the $M^{II}Fe^{III}$ compounds indicate the presence of antiferromagnetic ex-

(25) Coronado, E.; Gómez-García, C. J.; Nuez, A.; Romero, F. M.; Rusanov, E.; Stoeckli-Evans, H. *Inorg. Chem.* **2002**, *41*, 4615.
(26) Chernova, N. A.; Song, Y.; Zavalij, P. Y.; Wittingham, M. S. *Phys. Rev. B* **2004**, *70*, 144405.

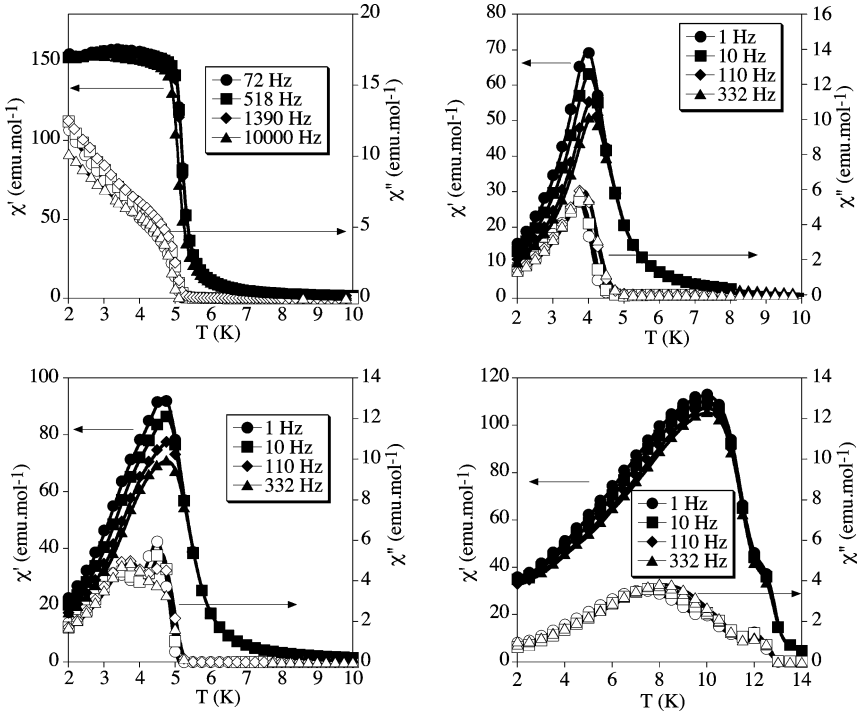

Figure 4. Frequency dependence of the in-phase ac susceptibility (χ', filled symbols) and out-of-phase AC susceptibility (χ'', empty symbols) of the IrMnCr (top left), IrFeCr (top right), IrCoCr (bottom left), and IrNiCr (bottom right) compounds.

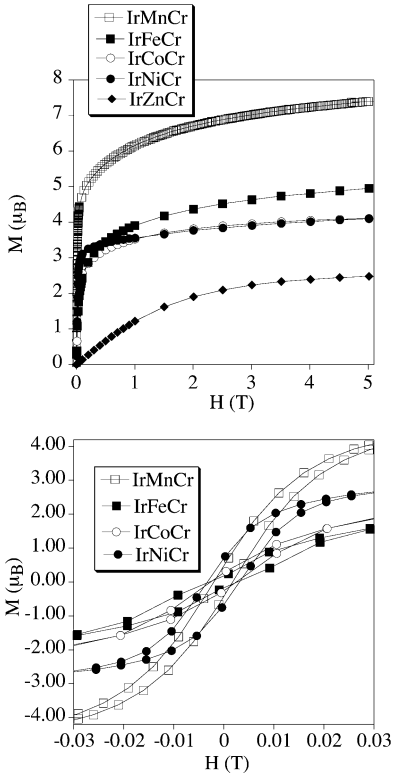

Figure 5. Field dependence of the magnetization (M) for the IrMCr series at 2 K (top). Hysteresis loop of magnetization of the IrMnCr, IrFeCr, IrNiCr, and IrCoCr compounds at 2 K (bottom).

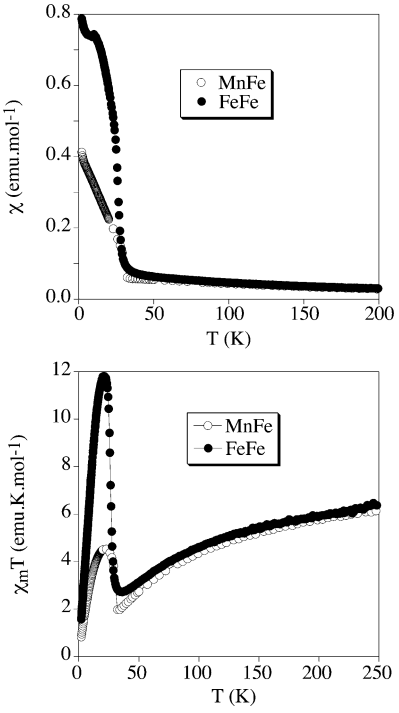

Figure 6. Temperature dependence of the magnetic susceptibility at 0.1 T (χ) for the IrMnFe and IrFeFe compounds (top). Temperature dependence of the χT product at 0.1 T for the IrMnFe and IrFeFe compounds (bottom).

change interactions (Figure 6). This behavior is analogous to that observed in the series $[Z^{II}(bpy)_3][ClO_4][M^{II}Fe(ox)_3]$ (M^{II} = Mn and Fe; Z^{II} = Fe and Ru).[17] Above ca. 50 K, the magnetic susceptibility of both compounds follows a Curie−Weiss law with large and negative Weiss constants, in agreement with the presence of antiferromagnetic interactions between neighboring ions.[3,17] At low temperatures, the two compounds exhibit a jump at ca. 30 K in both χ and χT. Below this jump, χ increases continuously and does not saturate (Figure 6, top). These features suggest the appearance of a magnetically ordered regime. This is confirmed by ac susceptibility measurements that show a sharp frequency-

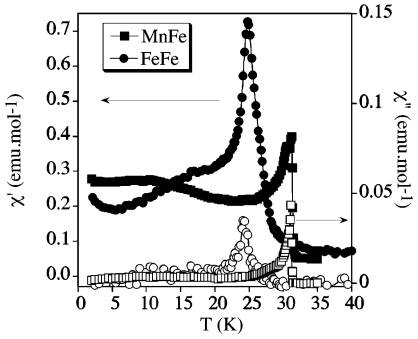

Figure 7. Temperature dependence of the out-of-phase ac susceptibility (χ'') and in-phase ac susceptibility (χ') for the IrMnFe and IrFeFe compounds at 10 Hz.

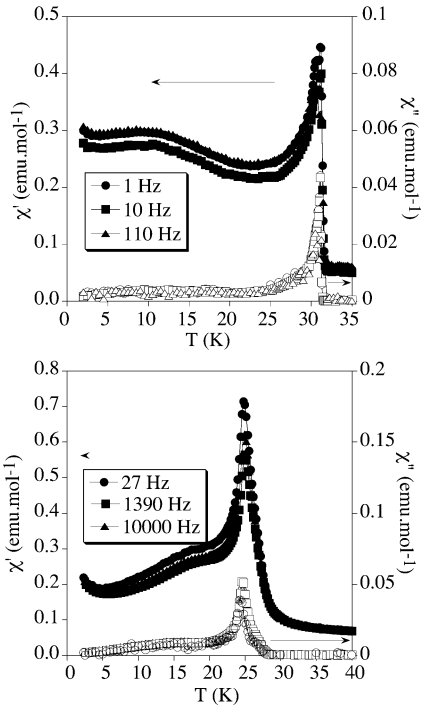

Figure 8. Frequency dependence of the in-phase ac susceptibility (χ', filled symbols) and out-of-phase ac susceptibility (χ'', empty symbols) of the IrMnFe (top) and IrFeFe (bottom).

independent maximum in χ' and χ''. The χ'' signal becomes nonzero at ca. 31 K for the MnFe compound and at ca. 28 K for the FeFe compound (Figure 7). The MnFe compound presents another frequency-independent peak in χ' at lower temperatures (Figure 8, top) which is also observed in the related $[Ru(bpy)_3][ClO_4][MnFe(ox)_3]$ compound and whose origin is unclear.[17] Taking into account the nature of interacting spins, the MnFe compound can be considered to be a weak ferromagnet in which the net magnetic moment comes from canting of the antiferromagnetically aligned $S(Mn^{II}) = S(Fe^{III}) = 5/2$ moments, while the FeFe compound can be considered to be a ferrimagnet due to the noncompensation of the antiferromagnetically coupled spins $S(Fe^{II}) = 2$ and $S(Fe^{III}) = 5/2$. Again, the magnetic behavior is similar to that of the $[Z^{II}(bpy)_3]^{2+}$ analogues but important increases in the critical temperatures are observed. Thus, the ordering temperature of the MnFe compound containing $[Ir(ppy)_2(bpy)]^+$ is higher by a factor of ca. 1.6−1.8 with respect to the $[Z^{II}(bpy)_3]^{2+}$ derivatives (31.0, 20.0, and 17.4 K for the Ir, Ru, and Fe derivatives, respectively). The same holds for the FeFe compound containing $[Ir(ppy)_2(bpy)]^+$ which shows a T_c higher by a factor of ca. 3.1−3.5 (28.0, 7.9, and 9.1 K for the Ir, Ru, and Fe derivatives, respectively).[17]

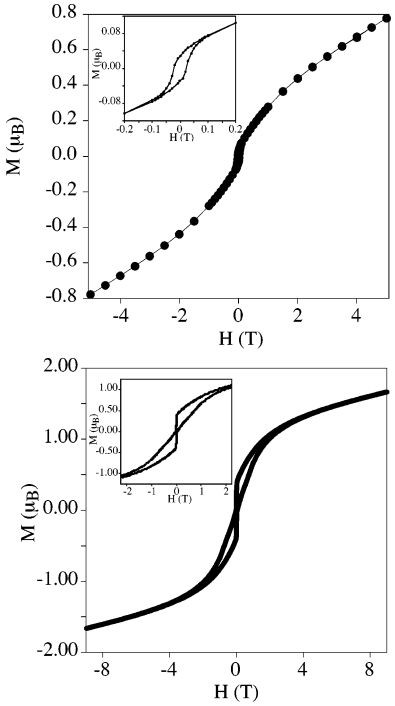

Figure 9. Hysteresis loop of magnetization at 2 K of the IrMnFe compound (top) and the IrFeFe compound (bottom).

In both compounds, the isothermal magnetization at 2 K shows an almost linear increase and is far from saturation at 5 T, as expected for an antiferromagnetic coupling (Figure 9). Both show hysteresis loops of the magnetization with coercive fields of 24 mT for MnFe and 30 mT for FeFe.

Magneto-structural Trends. From the above results, we can conclude that the $[Ir(ppy)_2(bpy)][M^{II}M^{III}(ox)_3]\cdot 0.5H_2O$ compounds and their $[Z^{II}(bpy)_3][ClO_4][M^{II}M^{III}(ox)_3]$ analogues present the same kind of magnetic interaction (ferromagnetic in the MCr series and antiferromagnetic in the MFe one) but with a significant increase in the ordering temperatures of the compounds reported in this work. The general trend if that the ordering temperatures have increased by a factor of 2 when passing from the series $[Z^{II}(bpy)_3][ClO_4][M^{II}Cr(ox)_3]$ to the series $[Ir(ppy)_2(bpy)][M^{II}Cr(ox)_3]$. A possible explanation of this behavior is connected with the shortening in both the unit cell and $M^{II}-M^{III}$ distances in the $[Ir(ppy)_2(bpy)]^+$ compounds due to the absence of the $[ClO_4]^-$ anion. This effect is clearly seen in Figure 10 where the *a* parameter and the ordering temperatures (T_c) are plotted for the different series of 3D compounds $[Ir(ppy)_2(bpy)][M^{II}Cr(ox)_3]\cdot 0.5H_2O$ and $[Z^{II}(bpy)_3][ClO_4][M^{II}Cr(ox)_3]$. An increase in the *a* parameter is observed when passing from $[Ir(ppy)_2(bpy)]^+$ to $[Fe(bpy)_3]^{2+}$, $[Ni(bpy)_3]^{2+}$, $[Co(bpy)_3]^{2+}$, and $[Ru(bpy)_3]^{2+}$, which can be correlated with the decrease in the ordering temperatures. The only exception is observed in the IrCoCr compound, whose ordering temperature is expected to be slightly higher (around 7 K, instead of 5.2 K).

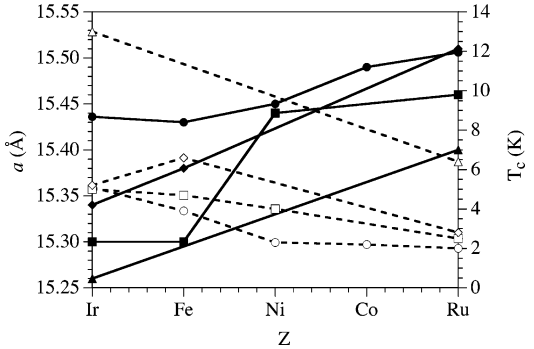

Figure 10. Variation of the *a* parameter (filled symbols, solid lines) and the ordering temperatures (T_c, empty symbols dashed lines) for the series of 3D compounds $[Ir(ppy)_2(bpy)][M^{II}Cr(ox)_3]\cdot 0.5H_2O$ and $[Z^{II}(bpy)_3][ClO_4][M^{II}Cr(ox)_3]$ with M^{II} = Mn (circles), Fe (squares), Co (rhombs), and Ni (triangles).

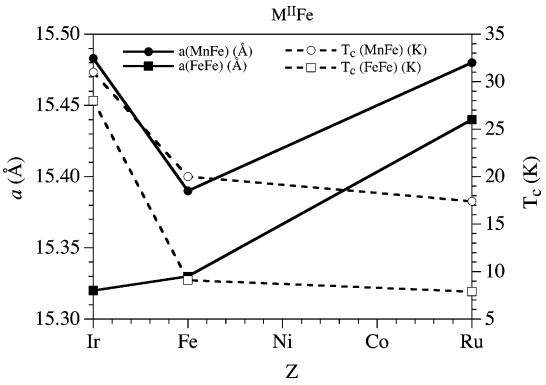

Figure 11. Variation of the *a* parameter (filled symbols, solid lines) and the ordering temperatures (T_c, empty symbols dashed lines) for the series of 3D compounds $[Ir(ppy)_2(bpy)][M^{II}Fe(ox)_3]\cdot 0.5H_2O$ and $[Z^{II}(bpy)_3][ClO_4][M^{II}Fe(ox)_3]$ with M^{II} = Mn (circles) and Fe (squares).

In the MFe compounds, the effect is quantitatively more pronounced and seems to follow the same trend as in the MCr series (i.e., increase in T_c when decreasing *a*), even if in the MFe series the $M^{II}-Fe$ coupling is antiferromagnetic (Figure 11). This effect can be seen in Tables 2 and 3 and Figure 11. Indeed, T_c increases by a factor up of 3 when the divalent cations $[Z^{II}(bpy)_3]^{2+}$ are changed by the monocation $[Ir(ppy)_2(bpy)]^+$, leading to the highest T_c values so far reported in the 3D bimetallic oxalate structure (31 K in the IrMnFe compound). The increase in T_c when decreasing *a* is not so clear in these series since the number of known examples is sensibly smaller than in the MCr series. Furthermore, there is a noteworthy exception to this trend in the MnFe series. In this case, the decrease in the *a* parameter when passing from IrMnFe (a = 15.483(6) Å) to FeMnFe (a = 15.39(3) Å) gives rise to a decrease (instead of the expected increase) in T_c (from 31.0 to 20 K) (Figure 11). These two features preclude to obtain a definite trend between the unit cell parameters and the ordering temperatures in the MFe series.

Conclusion

We have prepared the series of compounds of formulas $[Ir(ppy)_2(bpy)][M^{II}Cr(ox)_3]\cdot 0.5H_2O$ (M^{II} = Mn, Fe, Co, Ni, and Zn) and $[Ir(ppy)_2(bpy)][M^{II}Fe(ox)_3]\cdot 0.5H_2O$ (M^{II} = Mn and Fe). These compounds present the well-known 3D chiral structure already observed in the $[Z^{II}(bpy)_3][ClO_4]-[M^{II}M^{III}(ox)_3]$ series. The main difference between the two structures is that the presence of the $[Ir(ppy)_2(bpy)]^+$ monocation instead of the $[Z(bpy)_3]^{2+}$ dications makes unnecessary the presence of the charge-compensating $[ClO_4]^-$ anion in the holes left by the cation complexes and the oxalate network. The presence of a half a water molecule in the place of the $[ClO_4]^-$ anions reduces the unit cell volume with respect to the series $[Ru(bpy)_3][ClO_4][M^{II}M^{III}(ox)_3]$, even if the $[Ir(ppy)_2(bpy)]^+$ cation is bigger than $[Ru(bpy)_3]^{2+}$. This shortening in the unit cell parameters and in the intermetallic $M^{II}-M^{III}$ distances have significant consequences on the magnetic properties. In fact, the critical temperatures of these magnets have increased by a factor of ca. 2 and 3 in the $M^{II}Cr$ and $M^{II}Fe$ series, respectively, giving rise to the highest T_c's so far reported for the 3D oxalate compounds.

Given the chirality of these compounds, single crystals of them are very good candidates to study the presence of a magneto-chiral effect.[27] Another interesting feature of this family of compounds is the presence of the $[Ir(ppy)_2(bpy)]^+$ cation within the 3D oxalate network. This complex presents interesting luminescent properties that can give rise to photoinduced processes such as energy and electron transfer with the metallic ions of the oxalate network, as it has been observed for other 3D oxalate compounds.[28] The investigation of these aspects is in progress.

Acknowledgment. Financial support from the European Union (MERG-CT-2004-508033), the Spanish Ministerio de Educación y Ciencia (CTQ2005-09385-C03 project and MAT2004-03849 MEC grants), and Generalitat Valenciana is gratefully acknowledged. M.C.-L. thanks the Spanish Ministerio de Ciencia y Tecnología for a research contract (programa Ramón y Cajal).

Supporting Information Available: X-ray and heat capacity data. This material is available free of charge via the Internet at http://pubs.acs.org.

IC060442X

(27) Rikken, G. L. J. A.; Raupach, E. *Nature* **1997**, *390*, 493.
(28) (a) Decurtins, S.; Schmalle, H. W.; Pellaux, R.; Schneuwly, P.; Hauser, A. *Inorg. Chem.* **1996**, *35*, 1451. (b) Hauser, A.; Riesen, H.; Pellaux, R.; Decurtins, S. *Chem. Phys. Lett.* **1996**, *261*, 313. (c) von Arx, M. E.; Burattini, E.; Hauser, A.; van Pieterson, L.; Pellaux, R.; Decurtins, S. *J. Phys. Chem. A* **2000**, *104*, 883.